sustainability

MDPI

Article

Electrospun 3D Curly Electret Nanofiber Air Filters for Particulate Pollutants

Wei Zhao, Kelimu Tulugan *, Xin Zhang, Xiang Li and Peng Tian

School of Mechanical Engineering, Xinjiang University, Urumqi 830049, China; zhaowei202401@163.com (W.Z.); gum1hozhang@foxmail.com (X.Z.); 15649808856@163.com (X.L.); asd1016715897@163.com (P.T.)
* Correspondence: kelimu@xju.edu.cn

Abstract: Amidst rapid industrialization and urbanization, air pollution has emerged as a global environmental challenge. Traditional air filtration materials face challenges in effectively filtering PM0.3 and often result in discomfort due to high air resistance when used for personal protection, as well as excessive energy consumption in industrial air purification applications. This study initially utilized extremely high environmental humidity to induce fiber formation, resulting in the preparation of a fluffy fiber membrane with a three-dimensional curly morphology, which increased the porosity to 96.93%, significantly reducing air resistance during filtration. Subsequently, rutile TiO_2 with a high dielectric constant was introduced, exploiting the low pressure drop characteristic of the fluffy 3D curly fiber membrane combined with the electret effect of TiO_2 nanoparticles to notably improve the issue of excessive pressure drops while maintaining filtration efficiency. The microstructure, morphology, and element distribution of the fibers were analyzed using FESEM and EDS. FTIR and XRD were employed to examine the functional groups and crystal structure within the fibers. The electret effect and filtration performance of the fiber membrane were investigated using an electrostatic tester and a particulate filtration efficiency tester. The results demonstrated that inducing fiber formation under high-humidity conditions could produce fibers with a 3D curly structure. The fiber membrane was highly fluffy, significantly reducing the pressure drop. Introducing an appropriate amount of titanium dioxide markedly improved the electrostatic effect of the fiber membrane, enhancing the filtration performance of the 3D curly PVDF/TiO_2 composite fiber membrane. With a 0.5% addition of TiO_2 nanoparticles, the filtration efficiency of the fiber membrane reached approximately 99.197%, with a pressure drop of about 49.83 Pa. This study offers a new approach to developing efficient, low-resistance air filtration materials, showcasing the potential of material innovation in addressing air quality challenges within the sustainable development framework.

Keywords: curly fiber; high porosity; air filtration; electrospinning; individual protection; sustainability

check for updates

Citation: Zhao, W.; Tulugan, K.; Zhang, X.; Li, X.; Tian, P. Electrospun 3D Curly Electret Nanofiber Air Filters for Particulate Pollutants. *Sustainability* **2024**, *16*, 2808. https://doi.org/10.3390/su16072808

Academic Editor: Changhyun Roh

Received: 24 January 2024
Revised: 29 February 2024
Accepted: 26 March 2024
Published: 28 March 2024

Copyright: © 2024 by the authors. Licensee MDPI, Basel, Switzerland. This article is an open access article distributed under the terms and conditions of the Creative Commons Attribution (CC BY) license (https://creativecommons.org/licenses/by/4.0/).

1. Introduction

In light of the escalating environmental challenges, the issue of air quality has garnered significant attention [1]. The airborne particulate pollution resulting from the rapid advancement of industrial civilization, as well as the suspended dust caused by natural meteorological disasters such as sandstorms, have inflicted significant harm upon the ecological environment, public health, and industrial and agricultural productivity. Particularly in terms of health, these harmful particles can also harbor a multitude of viruses or bacteria, leading to the onset of various respiratory diseases and allergic symptoms in humans upon inhalation [2,3]. Tiny particles can penetrate human protective barriers, directly entering the lungs and even the bloodstream, as confirmed by scientific research. This has been closely associated with increased incidences of various health issues such as cardiovascular diseases and lung conditions. Researchers like Pope CA III have pointed out that prolonged exposure to PM pollution significantly increases the risk of mortality

from cardiovascular diseases [4]. In addition, gaseous pollutants in the atmosphere also introduce irritants to the human respiratory system, with prolonged exposure to them potentially exacerbating respiratory conditions such as asthma and chronic obstructive pulmonary disease. For instance, in Xinjiang, China, due to harsh natural conditions, occurrences of sandstorms increase, resulting in higher levels of particulate matter in the atmosphere, which significantly elevates the incidence of tuberculosis in Xinjiang compared to other regions [5].

Traditional air filtration materials struggle to effectively filter PM0.3 particles and typically exhibit high air resistance, leading to breathing difficulties when used in masks [6]. Air filtration materials with excessively high pressure drops will also lead to excessive energy consumption when used in industrial air purification systems [7]. In order to protect the public from harmful particles and reduce the energy consumption of air filters, we must persistently develop high-efficiency and low-resistance air filters.

Electrospinning technology is an advanced process for preparing nanofiber membranes. Polymer materials or other material solutions are sprayed into nano- to micron-sized fibers by using electrostatic [8]. The fabrication of nanofibers through electrospinning offers the advantages of being relatively straightforward, efficient, controllable, and facile to produce [9]. In general, the greater the porosity of a nanofiber membrane, the more superior its permeability and adsorption capabilities. Therefore, high specific surface area and elevated porosity are crucial for the preparation of high-performance nanofiber membranes [10,11].

Three-dimensional curly nanofibers possess a substantial specific surface area owing to their distinctive morphology [12]. A curly nanofiber membrane has a fluffy structure, a high porosity that allows molecules and ions to pass through effectively, and a large surface area that provides a large number of reaction and adsorption sites; it also has wide application potential in filtration, sensing, biomedicine, and composite materials [9,13–15]. Its curly structure can also increase its mechanical strength and toughness, making it more durable and reliable in its applications [16]. Therefore, the preparation of nanofiber membranes with high porosity and a 3D curly structure is a promising research direction with broad application prospects [15,17,18]. TiO_2 NPs not only have excellent photocatalysis and corrosion resistance but are also a metal oxide with a high dielectric constant [19–21]; TiO_2 is often used to increase dielectric constants [22–24]. Studies have shown that TiO_2 NPs can be compounded with PVDF-TIFE, which proves that the introduction of TiO_2 NPs can greatly improve the dielectric constant of the material, and the effect of rutile TiO_2 NPs is better than that of anatase TiO_2 NPs. Daehwan Cho et al. found that TiO_2 NPs were added to the polypropylene (PAN) electrospinning membrane by electrospinning and that the PAN electrospinning membrane had larger pore sizes and wider pore size distributions. However, when filtering fine particles, the TiO_2/PAN electrospinning membrane shows better filtration efficiency than the pure PAN electrospinning membrane. This is due to the addition of TiO_2NPs, which improves the charging ability of the PAN electrospinning membrane [25].

In this paper, we successfully prepared 3D curly nanofibers by using the extremely high humidity of the spinning environment to induce fiber formation and realized the highly fluffy accumulation of the electrospinning membrane. Subsequently, the electret-reinforced TiO_2 NPs particles were doped into it, and the prepared electret-reinforced nanofibers still maintained a 3D curly structure, forming a highly fluffy nanofiber membrane. We studied the influence of the mass ratio of TiO_2 NPs in PVDF/TiO_2 on the microstructure and the electret effect of 3D curly nanofibers and tested their air filtration performance, which provided some basic research for preparing high-efficiency and low-resistance air filtration nanofiber membranes with an electret effect. Low pressure drops will ensure the comfort of individuals wearing personal respiratory protective air filters for extended periods. It is expected to reduce energy consumption when applied in industrial air purification systems, demonstrating the potential of material innovation to address air quality challenges within the framework of sustainable development.

2. Materials and Methods

2.1. Materials

Polyvinylidene fluoride powder (PVDF, Mw = 500,000) was purchased from Arkema (Colombes, France). Nanometer titanium dioxide particles (TiO_2 NPs) with an average particle size of 100 nm and purity of 99.9% were obtained from Shanghai Macklin Biochemical Technology Co., Ltd. (Shanghai, China). *N*,*N*-Dimethylacetamide (DMF, purity > 99.8%) and Tetrahydrofuran (THF, purity > 99%) were supplied by Shanghai Aladdin Bio-Chem Technology Co., Ltd., China (Shanghai, China).

2.2. Electrospinning Process

Take a suitable quantity of PVDF powder and position it in an electric constant-temperature blast drying oven for 2 h prior to usage. Introduce a specific amount of TiO_2 NP powder into a blended solvent of DMF and THF with a mass ratio of 1:1. Following magnetic stirring for 1 h, employ ultrasonic vibration for 30 min, then incorporate PVDF to form a PVDF solution with a mass fraction of 13 wt%, and stir for 8 h until the solution is uniformly mixed. Subsequently, transfer the spinning solution to a syringe equipped with a metal nozzle (inner diameter of 0.7 mm), set the distance from the needle to the drum receiver at 16 cm, maintain the solution feed rate at 1 mL/h, and set the spinning voltage to 20 kV.

Prepare the spinning solution according to the above operation and perform the spinning according to the parameters in the table. The obtained nanofiber samples are recorded in order as L-P, H-P, H-P/T1, H-P/T2, H-P/T3, and H-P/T4. The configuration of the electrospinning precursor solution and spinning parameters are shown in the following Table 1.

Table 1. Membranes and corresponding parameters.

Membrane	PVDF (wt%)	TiO_2 NPs (wt%)	DMF:THF (wt%)	Relative Humidity (RH%)
L-P	13	0	1:1	40
H-P	13	0	1:1	95
H-P/T1	13	0.25	1:1	95
H-P/T2	13	0.5	1:1	95
H-P/T3	13	0.75	1:1	95
H-P/T4	13	1.0	1:1	95

2.3. Characterization

The JSM-7610F Plus field emission scanning electron microscope (FESEM, JEOL Ltd., Akishima, Japan) was utilized for observing and analyzing the micro-surface morphology of the curly nanofiber membrane. The fiber diameter distribution was estimated by the statistical analysis of 200 fibers randomly selected using image analysis software (ImageJ, https://imagej.net/ij/). The relative humidity in the process of electrospinning is measured with a temperature and humidity tester. Horiba's EDS energy spectrometer was employed to conduct qualitative and quantitative analyses of the surface distribution of C, H, F, and other elements on the PVDF/TiO_2 nanofiber membrane, and to detect the impact of adding different contents of TiO_2 on the element distribution of the PVDF nanofiber membrane and the effects of each element proportion. The phase structure and related crystal planes were examined using BRUKER's D8 Advance X-ray diffractometer. Perkinelmer's TM900H Fourier transform infrared spectrometer (FTIR, PerkinElmer, Waltham, MA, USA) was utilized to detect information such as chemical bond type, molecular structure, functional group content, and the molecular interaction of PVDF/TiO_2 mass fraction. DR251XL Particles filtration efficiency tester (Darong, Ningbo, China) tests the filtration efficiency and pressure drop of the fiber membranes.

3. Results and Discussion

3.1. FESEM Analysis

The humidity of the electrospinning environment impacts the evaporation of the solvent, thus influencing the solidification process of the spinning jet into fibers. It stands as one of the pivotal factors in the electrospinning process. The electron microscope images depicting the morphology of PVDF nanofiber membranes prepared through electrospinning in environments with low humidity (40RH%) and high humidity (95RH%) are illustrated in Figure 1.

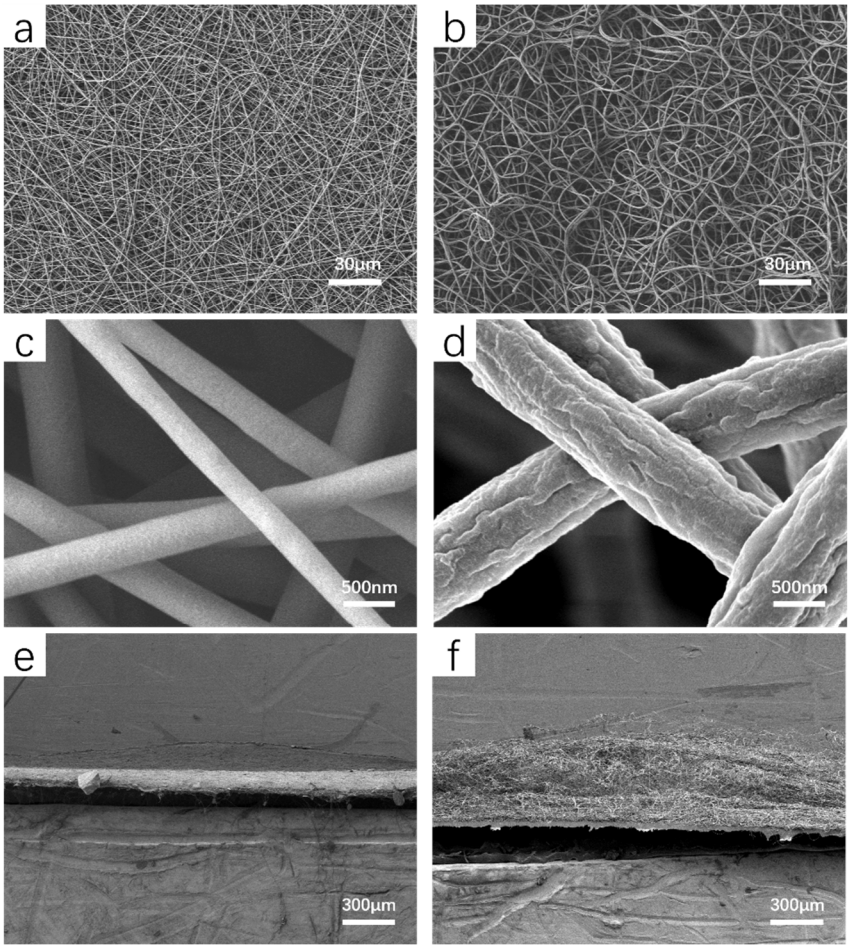


Figure 1. PVDF nanofibers from 40RH%: (**a**) L-P fibers are observed to be straight at 500×; (**c**) L-P fibers are smooth surface observed at 30,000×; (**e**) seen from the side, L-P fiber membranes are densely packed. PVDF nanofibers from 95RH%: (**b**) H-P fibers are observed to be 3D curly at 500×; (**d**) H-P fibers are rough surface observed at 30,000×; (**f**) seen from the side, the H-P fiber membrane is very fluffy.

According to Figure 1a, it is evident that PVDF nanofibers fabricated in a low-humidity environment exhibit a uniform distribution in a typical linear morphology, with the fiber surface appearing remarkably smooth at the microscopic level, as depicted in Figure 1c. However, as the humidity exceeds 95RH%, the structure of the fabricated PVDF nanofibers undergoes significant changes. As per Figure 1b, the nanofibers exhibit a 3D curly morphology. Upon comparing Figure 1b with Figure 1d, it becomes apparent that the fiber surface prepared in a high-humidity environment is rougher. Figure 1e,f represent side views of the two samples, respectively. It is observable that the fiber membrane prepared in a low-humidity environment forms a densely packed membrane, while the fiber mem-

brane prepared in an ultra-high-humidity environment assumes a highly voluminous 3D curly structure.

According to the FESEM analysis, relative humidity is a crucial factor that influences the 3D structure of electrospinning, benefiting from the favorable interaction between water and solvent. A high concentration of water molecules will enhance solvent evaporation and modulate the exchange rate between water molecules and DMF, thereby directly impacting the trajectory of the jet and, consequently, the morphology of the nanofibers deposited on the receiving substrate. At a humidity level of 95%, the weak electric field force during stretching will induce residual stress in the polymer network structure, leading to the retraction of highly intertwined molecular chains. This phenomenon results in the observation of curly fibers when spinning in a high-humidity environment [26,27]. According to Figure 1b,d, it is evident that the fiber surface prepared in a low-humidity environment appears smooth under microscopic observation, while the surface of the PVDF nanofiber prepared in a high-humidity environment exhibits irregular gullies and a rougher texture. This phenomenon may be attributed to the accelerated evaporation of the DMF solvent in the spinning jet in a high-humidity environment. The DMF solvent rapidly volatilizes and absorbs heat during the drawing process, causing a decrease in the jet temperature, which leads to the condensation of water vapor on the fiber surface, forming water droplets [28].

The process comprises a large amount of water vapor contained in the air being uniformly dispersed in the space in the form of atomized nano-scale droplets, and the droplets formed by condensation and the nano-scale droplets in the space in a high-humidity environment will occupy the space on the fiber surface; after the fiber is completely dried, the droplets evaporate from the liquid to the air, vacating the original space, forming pits, and finally the PVDF fiber with rough surface appears.

When the fiber membrane is utilized for filtration, the 3D curly fiber structure can result in reduced air resistance. However, the space support effect brought about by this 3D curly structure will also marginally decrease the filtration efficiency of the fiber membrane. It is generally considered an effective strategy to enhance filtration efficiency by imparting an electrostatic electret effect to the nanofiber filter without compromising the filter pressure drop. In line with this perspective, TiO_2 NPs were introduced into the spinning solution as an electret enhancer, and PVDF nanofibers with an electret effect were prepared in a single step through electrostatic spinning. Figure 2 shows the SEM images of PVDF/TiO_2 composite nanofibers with TiO_2 NP contents of 0.25 wt%, 0.5 wt%, 0.75 wt%, and 1.0 wt%. In comparison with pure PVDF in Figure 1b, the introduction of 0.25 wt% and 0.5 wt% TiO_2 NPs appears to have no effect on the crimp morphology, and with the addition of TiO_2 NPs, the fiber diameter decreases slightly in Figure 3. This may be attributed to the incorporation of TiO_2 NPs, causing the solution to carry more charges, and the fibers are drawn thinner under the action of the electric field stretching. However, if the content of nano-titanium dioxide is further increased, the curling phenomenon of the nanofibers will weaken or even disappear, and the nano-titanium dioxide particles will also agglomerate. The weakening and disappearance of the curly structure may reduce the porosity of the fiber, and the increase in agglomeration may lead to uneven charge distribution, and it even has the reunion fall off.

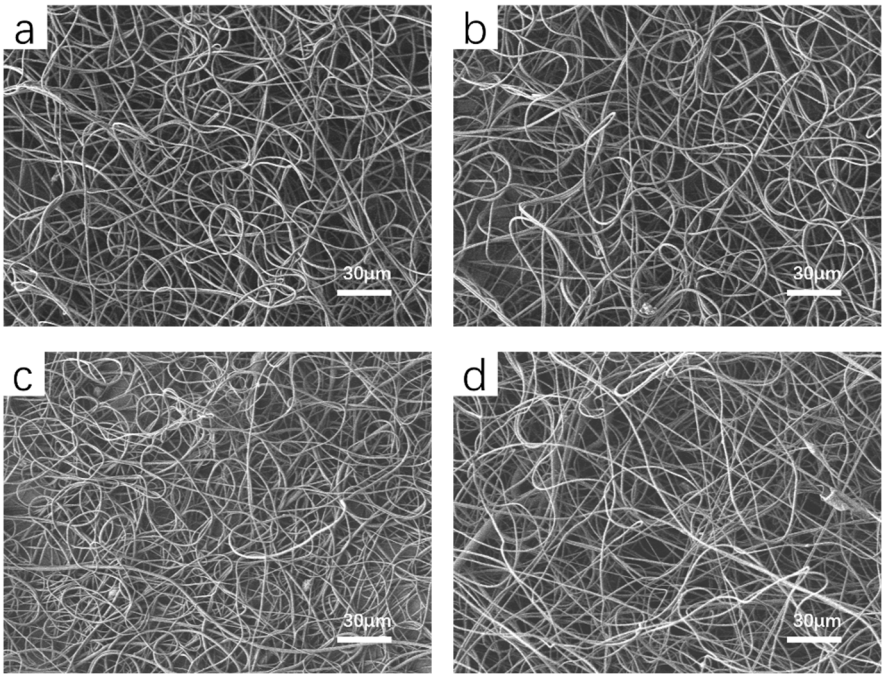


Figure 2. PVDF/TiO_2 nanofibers from 95RH%: (**a**) H-P/T1, (**b**) H-P/T2, (**c**) H-P/T3, and (**d**) H-P/T-4.

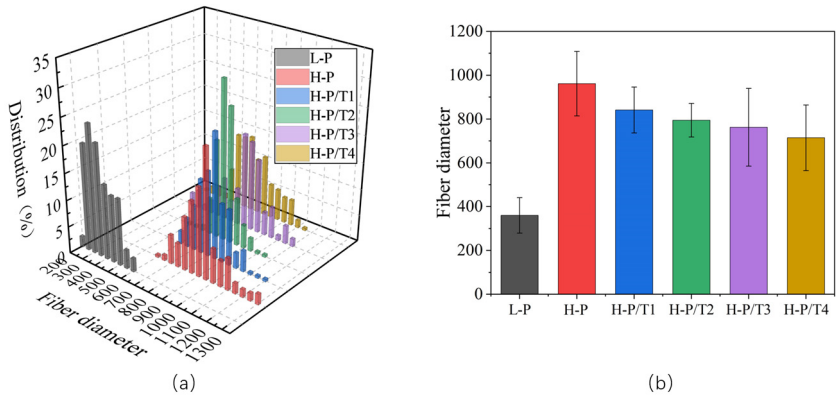


Figure 3. Diameter distribution and average diameter of fibers. (**a**) Comparison chart of fiber membrane diameter distribution. (**b**) Comparison chart of fiber average diameter.

3.2. EDS Analysis of 3D Curly Fiber Membranes

Figure 4 shows the EDS element distribution diagram of a 3D curly nanofiber composite membrane with a mass fraction of 0.5 wt% added TiO_2 electret particles. The C, O, F, and Ti elements are marked in red, yellow, green, and purple, respectively. By combining Figure 4 and Table 2, it can be seen that the proportion of the C and F elements is relatively high. The fiber outline can be slightly observed through the C and F element distribution diagram. This is because the fiber-based material PVDF is dominated by C elements and F elements. The O element occupies a low proportion, and the Ti element occupies the lowest proportion. It is almost impossible to see the fiber outline from the element distribution of O and Ti, and it shows that O and Ti elements are evenly distributed on the nanofiber membrane. The electret particle TiO_2 NP was successfully compounded on 3D curly nanofibers.

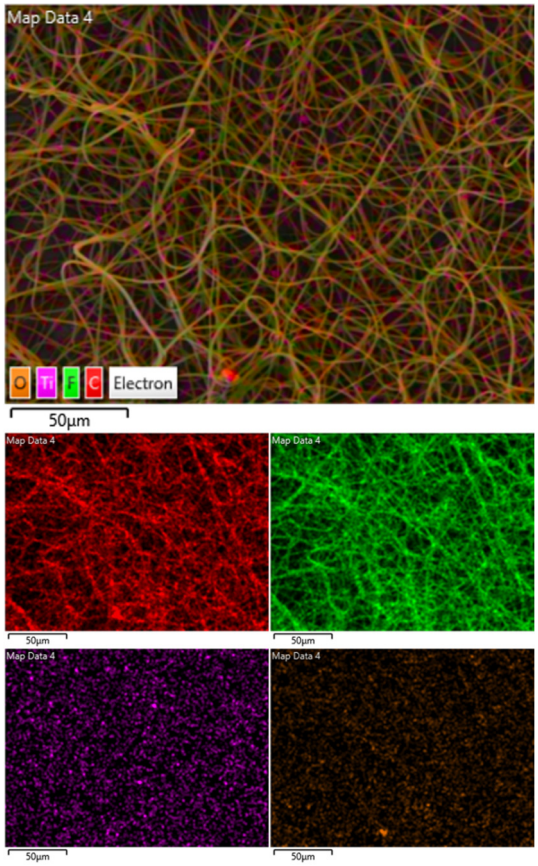


Figure 4. EDS of H-P/T2 composite 3D curly nanofiber membranes.

Table 2. The element content of PVDF/TiO_2 composite 3D curly fiber membranes of H-P/T2.

Element	C	O	F	Ti
wt%	42.6	1.87	54.61	0.92

3.3. FTIR Analysis Nanofiber Membranes

Figure 5 shows FTIR spectra of different nanofiber membranes, respectively. At 1401 cm^{-1}, there is the stretching vibration absorption peak of CH2 [29]. At 1274 cm^{-1} and 1177 cm^{-1} there are peaks due to the symmetrical and asymmetrical stretching of CF2, which are the main peaks in PVDF and represents the fluoride part in PVDF. At 1071 cm^{-1}, the vibration of CF2 indicates a special bending vibration of fluoride groups [30]. At 876 cm^{-1}, there is one of the characteristic peaks of PVDF; the peak at 836cm^{-1} is the bending vibration absorption peak of the CH bond [31]. For the Ti-O stretching vibration, a new broad characteristic absorption peak appears in the range of 500–800 cm^{-1}, which may appear as one or more peaks. The tensile vibration of the O-Ti-O bond in doped TiO_2 is the main reason for the appearance of additional peaks and peak shifts. It shows that TiO_2 NP was successfully compounded into PVDF nanofibers.

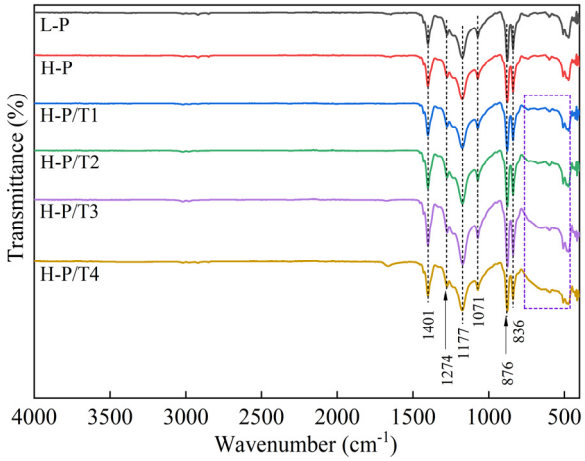


Figure 5. FTIR spectrum of fiber membrane.

3.4. XRD Analysis Nanofiber Membranes

The morphology of the membranes was studied using X-ray diffraction patterns as shown in Figure 6. PVDF has been found so far to crystallize in five polymorphs and forms [32], but mainly in α, β, and γ forms [33]. The diffraction peak at the diffraction angle of 18.5° is the α phase (020) crystal plane, and the diffraction peak at the diffraction angle of 20.6° corresponds to the β phase [34]. The XRD patterns of H-P and L-P fiber membranes are almost the same, indicating that ultra-high environmental humidity has little effect on the crystal form of the prepared 3D curly PVDF nanofibers.

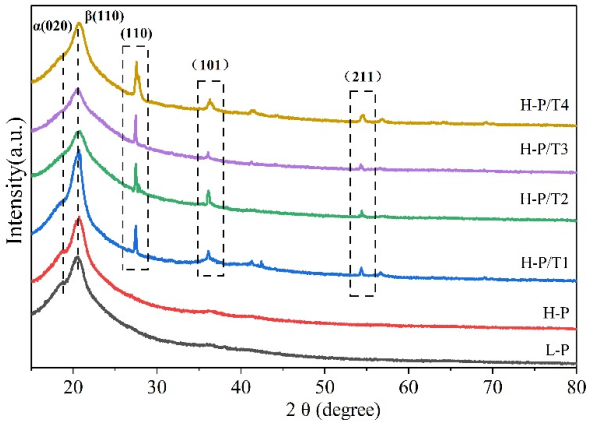


Figure 6. XRD patterns of fiber membrane.

H-P/T1, H-P/T2, H-P/T3, and H-P/4 fiber membranes produced new rutile TiO_2 diffraction peaks at 27.4°, 36.1°, and 54.4°, confirming that TiO_2 NP was introduced into the fiber membranes [35]. As the TiO_2 NP content increases, the α phase diffraction peak of PVDF gradually becomes weaker, indicating that the addition of TiO_2 NPs may inhibit the generation of the α phase of PVDF.

3.5. Nanofiber Membrane Surface Electret Effect

Based on the dominant dipole charge in PVDF fiber, the surface potential of the fiber membrane is negative [36]. Each sample was tested at 20 points. Figure 7 shows that the surface potential of densely packed PVDF nanofiber membrane (P-L) prepared in a low-humidity environment is about −6.42 kV.

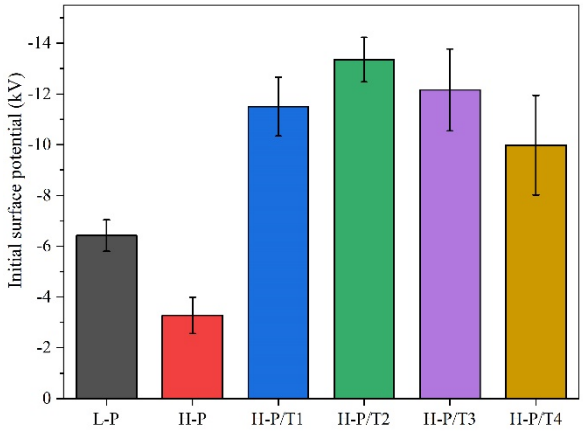


Figure 7. Fiber membranes surface electret effect.

The surface potential of the 3D curly PVDF nanofiber membrane (H-L) prepared in a high-humidity environment is significantly reduced. This may be due to the fact that when the nanofibers are prepared in a high-humidity environment, water molecules in the air take away part of the charge, causing the resulting nanofibers to have a reduced charge.

After adding electret particle TiO_2 NPs, the surface potential of the 3D curly nanofiber membrane increased significantly. This is because the addition of TiO_2 NPs increased the area between the crystalline and amorphous regions and introduced polar groups. The Maxwell–Wagner effect is caused by the interface between PVDF and TiO_2 NPs [37,38]. The charges in PVDF and TiO_2 NPs will move in the same direction under the action of an external electric field. Due to the different charge transport capabilities of PVDF and TiO_2 NPs, a charge barrier is generated at the interface, making it difficult for the charges to transfer at the interface. Accumulate to form interface charges [39], it can be seen from the XRD pattern that the addition of TiO_2 NPs also affects the crystal phase formation of PVDF fiber, which may also be another reason for its better performance in terms of electret effect. With the increase of TiO_2 content, the electret effect decreases, which may be due to the formation of charge channels due to the aggregation of TiO_2, resulting in uneven charge distribution and decreased charge storage capacity, but it is still significantly higher than that of H-P a fibrous membrane without adding TiO_2.

3.6. Porosity of Nanofiber Membranes

Compared with ordinary woven materials, electrospinning membranes have higher porosity, but most of them are dense fiber membranes like L-P fiber membranes.

The porosity of the fiber membrane was evaluated by the following formula:

$$P = \frac{V_0 - V}{V_0}$$

where V_0 represents the volume of the membrane in its natural state, and V refers to the absolute dense volume of the material. Because V_0 and V are not easy to obtain directly, it is deduced from the following formula:

$$P = 1 - \frac{m}{\rho S h}$$

where m represents the quality of the membrane, which is measured by a high-precision electronic scale; ρ denotes the density of raw materials; S represents the area of the sample membrane; and h represents the thickness of the membrane that was obtained based on the SEM images of side views.

As shown in Figure 8, the porosity of a L-P fiber membrane is close to 70%. As can be seen intuitively from Figures 1 and 2, a 3D curly fiber membrane has a highly fluffy

structure, and this special spatial structure brings higher porosity. Compared with the tightly packed L-P fiber membrane, the porosity of a fluffy 3D curly fiber membrane is greatly improved. Due to the good supporting effect of 3D crimped fibers and electrostatic repulsion between fibers, the porosity of an H-P fiber membrane reaches about 96.93%. This result is consistent with the side-view results of L-P (densely packed membrane) and H-P (fluffy membrane) shown in Section 3.1. The gap between fibers of the 3D curled membrane is larger, which will be beneficial to the electret effect. After the introduction of titanium dioxide nanoparticles, the porosity decreased slightly, but it was still significantly higher than that of L-P fiber membrane.

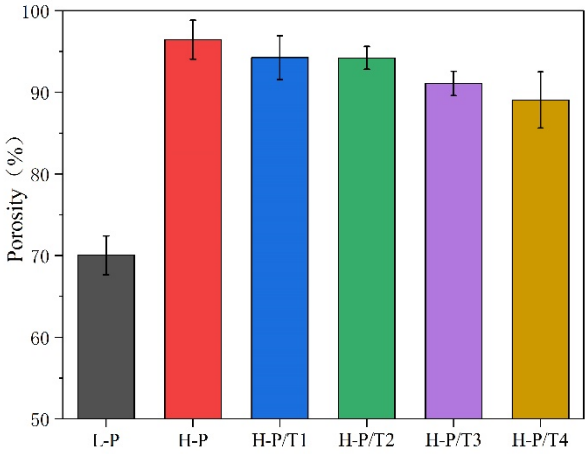


Figure 8. Membrane porosity.

3.7. Filtration Performance of Nanofiber Membranes

In order to further study the filtration performance of the prepared nanofiber membrane, $PM_{0.3}$ is selected as the filtered particulate matter. The results are shown in Figure 9. The filtration efficiency of PVDF nanofiber membrane (L-P) prepared in a low-humidity environment is about 92.63%, and the pressure drop is about 80.5 Pa. Due to the fluffy structure of the three-dimensional curled fiber membrane, the fiber scaffold has a very high porosity, and a space scaffold structure is formed between the fibers. The airflow can more easily pass through the fiber membrane, and the filtration pressure drop of the H-P fiber membrane is significantly reduced. But, its filtration efficiency is seriously reduced, because the electrostatic adsorption effect of the H-P fiber membrane prepared in a high-humidity environment is low, the fiber is fluffy and the pore size is too large, and the mechanical filtration in PVDF fiber membrane is dominant in this case. After the introduction of electret-enhanced particle TiO_2 NPs, the filtration efficiency is significantly improved.

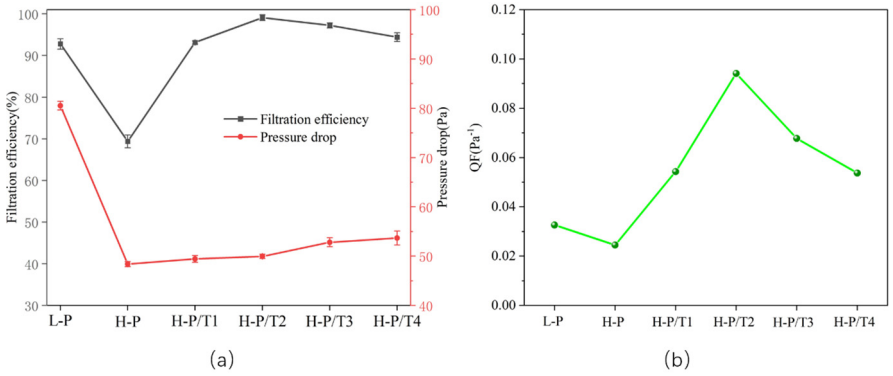


Figure 9. (**a**) Filtration efficiency and pressure drop. (**b**) Quality factor (QF).

With the increase in TiO_2 NP content, the filtration efficiency increased from 70.1% to 99.197%. On the one hand, this is attributed to the decreases in the diameter and pore

sizes of nanofibers after adding TiO_2, and the slight increase in particles intercepted on the fiber surface and adsorbed inside the fiber through gravity sedimentation and diffusion effects. On the other hand, with the addition of TiO_2, the initial surface potential of the fiber membrane improves the ability of the fiber membrane to store space charges and polarized charges and then improves the electrostatic adsorption ability of the fiber membrane. In this case, the electrostatic effect is dominant.

As particles pass through the nanofiber membrane, they are intercepted and adsorbed by the fiber membrane under the influence of the sum of the interception effect, Brownian diffusion, gravity effect, inertial impaction, and electrostatic deposition [40,41], and, thus, greatly improving the filtration performance of the fiber membrane. When the content of TiO_2 increased from 0 wt% to 0.5 wt%, the filtration performance of the fiber membrane showed an upward trend, and the quality factor reached about 0.096 at 0.5 wt%.

When the TiO_2 NP content is further increased, a decrease in filtration efficiency can be observed, which may be because the aggregation of TiO_2 NPs reduces the electrostatic adsorption effect of the nanofiber membrane. And when the TiO_2 NP mass fraction increases to 1 wt%, it significantly affects the morphology of the fiber, reduces the uniformity of the fiber membrane, and, thus, affects the filtration performance of the electrospinning membrane.

4. Conclusions

In this article, 3D curly nanofibers were prepared by electrostatic spinning in a high-humidity environment above 95RH%. Compared with the densely packed nanofiber membrane prepared in a normal-humidity environment, the 3D curly nanofibers formed a highly fluffy nanofiber membrane, and its filter pressure drop decreased significantly. A suitable quantity of TiO_2 NPs was incorporated as an electret reinforcement to fabricate a highly voluminous 3D curly PVDF/TiO_2 nanofiber membrane. The element distribution, functional groups, and element content on the surface of the fiber membrane were analyzed by EDS, FTIR, and XRD, which showed that TiO_2 NPs had been successfully compounded on PVDF fiber. It provides some basic research for PVDF/TiO_2 composite fiber membranes. The doping of a small amount of TiO_2 NPs has no obvious influence on the 3D curly fluffy structure. The addition of electret particle TiO_2 NPs obviously enhances the electrostatic adsorption of the fiber membrane, greatly improves the electrostatic effect in the process of fiber membrane filtration, and improves the filtration efficiency of 3D curly nanofiber membranes. The filtration efficiency of the H-P/T2 fiber membrane with a TiO_2 NP addition amount of 0.5 wt% is about 99.197%, and the pressure drop is about 49.83 Pa.

The 3D curled nanofiber membrane prepared in this study can not only significantly improve the comfort and efficiency of personal protective equipment but it also reduces energy consumption in the field of industrial air purification, showing the great potential of material innovation in meeting the global air quality challenges and promoting sustainable development.

Author Contributions: Conceptualization, W.Z. and K.T.; methodology, W.Z.; validation, W.Z., X.L. and P.T.; investigation, X.Z.; resources, K.T.; data curation, W.Z.; writing—original draft preparation, W.Z.; writing—review and editing, W.Z.; visualization, W.Z.; supervision, K.T.; project administration, K.T.; funding acquisition, K.T. All authors have read and agreed to the published version of the manuscript.

Funding: This research was funded by the Natural Science Foundation of the Xinjiang Uygur Autonomous Region, grant number (2021D01C101).

Institutional Review Board Statement: Not applicable.

Informed Consent Statement: Not applicable.

Data Availability Statement: The data presented in this study are available upon request from the corresponding author.

Conflicts of Interest: The authors declare no conflicts of interest.

References

1. Heal, M.R.; Kumar, P.; Harrison, R.M. Particles, Air Quality, Policy and Health. *Chem. Soc. Rev.* **2012**, *41*, 6606–6630. [CrossRef] [PubMed]
2. Feng, T.; Sun, Y.; Shi, Y.; Ma, J.; Feng, C.; Chen, Z. Air Pollution Control Policies and Impacts: A Review. *Renew. Sustain. Energy Rev.* **2024**, *191*, 114071. [CrossRef]
3. Ebenstein, A.; Fan, M.; Greenstone, M.; He, G.; Yin, P.; Zhou, M. Growth, Pollution, and Life Expectancy: China from 1991–2012. *Am. Econ. Rev.* **2015**, *105*, 226–231. [CrossRef]
4. Pope, C.A., 3rd; Ezzati, M.; Dockery, D.W. Fine-Particulate Air Pollution and Life Expectancy in the United States. *N. Engl. J. Med.* **2009**, *360*, 376–386. [CrossRef] [PubMed]
5. Zhang, Y.; Wang, X.; Liu, N.; Wang, S.; Wang, X.; Cao, M. Intervention Effect of New Tuberculosis Control Model on Tuberculosis Incidence in Xinjiang. *Infect. Drug Resist.* **2023**, *16*, 7485–7496. [CrossRef] [PubMed]
6. Afshari, A.; Ekberg, L.; Forejt, L.; Mo, J.; Rahimi, S.; Siegel, J.; Chen, W.; Wargocki, P.; Zurami, S.; Zhang, J. Electrostatic Precipitators as an Indoor Air Cleaner—A Literature Review. *Sustainability* **2020**, *12*, 8774. [CrossRef]
7. Fisk, W.J.; Faulkner, D.; Palonen, J.; Seppanen, O. Performance and Costs of Particle Air Filtration Technologies. *Indoor Air* **2002**, *12*, 223–234. [CrossRef] [PubMed]
8. Bhardwaj, N.; Kundu, S.C. Electrospinning: A Fascinating Fiber Fabrication Technique. *Biotechnol. Adv.* **2010**, *28*, 325–347. [CrossRef] [PubMed]
9. Luraghi, A.; Peri, F.; Moroni, L. Electrospinning for Drug Delivery Applications: A Review. *J. Control. Release* **2021**, *334*, 463–484. [CrossRef]
10. Shao, Z.; Chen, H.; Wang, Q.; Kang, G.; Wang, X.; Li, W.; Liu, Y.; Zheng, G. High–Performance Multifunctional Electrospun Fibrous Air Filter for Personal Protection: A Review. *Sep. Purif. Technol.* **2022**, *302*, 122175. [CrossRef]
11. Zhu, F.; Zheng, Y.-M.; Zhang, B.-G.; Dai, Y.-R. A Critical Review on the Electrospun Nanofibrous Membranes for the Adsorption of Heavy Metals in Water Treatment. *J. Hazard. Mater.* **2021**, *401*, 123608. [CrossRef] [PubMed]
12. Sun, B.; Long, Y.; Zhang, H.; Li, M.; Duvail, J.; Jiang, X.; Yin, H. Advances in Three-Dimensional Nanofibrous Macrostructures via Electrospinning. *Prog. Polym. Sci.* **2014**, *39*, 862–890. [CrossRef]
13. Blakeney, B.A.; Tambralli, A.; Anderson, J.M.; Andukuri, A.; Lim, D.-J.; Dean, D.R.; Jun, H.-W. Cell Infiltration and Growth in a Low Density, Uncompressed Three-Dimensional Electrospun Nanofibrous Scaffold. *Biomaterials* **2011**, *32*, 1583–1590. [CrossRef] [PubMed]
14. Jeong, S.I.; Burns, N.A.; Bonino, C.A.; Kwon, I.K.; Khan, S.A.; Alsberg, E. Improved Cell Infiltration of Highly Porous 3D Nanofibrous Scaffolds Formed by Combined Fiber–Fiber Charge Repulsions and Ultra-Sonication. *J. Mater. Chem. B* **2014**, *2*, 8116–8122. [CrossRef] [PubMed]
15. Lee, S.; Joshi, M.K.; Tiwari, A.P.; Maharjan, B.; Kim, K.S.; Yun, Y.-H.; Park, C.H.; Kim, C.S. Lactic Acid Assisted Fabrication of Bioactive Three-Dimensional PLLA/β-TCP Fibrous Scaffold for Biomedical Application. *Chem. Eng. J.* **2018**, *347*, 771–781. [CrossRef]
16. Li, Y.; Cao, L.; Yin, X.; Si, Y.; Yu, J.; Ding, B. Ultrafine, Self-Crimp, and Electret Nano-Wool for Low-Resistance and High-Efficiency Protective Filter Media against PM0. 3. *J. Colloid. Interface Sci.* **2020**, *578*, 565–573. [CrossRef] [PubMed]
17. Hwang, T.I.; Maharjan, B.; Tiwari, A.P.; Lee, S.; Joshi, M.K.; Park, C.H.; Kim, C.S. Facile Fabrication of Spongy Nanofibrous Scaffold for Tissue Engineering Applications. *Mater. Lett.* **2018**, *219*, 119–122. [CrossRef]
18. Vaquette, C.; Cooper-White, J.J. Increasing Electrospun Scaffold Pore Size with Tailored Collectors for Improved Cell Penetration. *Acta Biomater.* **2011**, *7*, 2544–2557. [CrossRef] [PubMed]
19. Diebold, U. The Surface Science of Titanium Dioxide. *Surf. Sci. Rep.* **2003**, *48*, 53–229. [CrossRef]
20. Zhang, M.; Wang, Y.; Zhang, Y.; Song, J.; Si, Y.; Yan, J.; Ma, C.; Liu, Y.-T.; Yu, J.; Ding, B. Conductive and Elastic TiO_2 Nanofibrous Aerogels: A New Concept toward Self-Supported Electrocatalysts with Superior Activity and Durability. *Angew. Chem. Int. Ed.* **2020**, *59*, 23252–23260. [CrossRef]
21. Rudakova, A.V.; Emeline, A.V.; Romanychev, A.I.; Bahnemann, D.W. Photoinduced Hydrophilic Behavior of TiO_2 Thin Film on Si Substrate. *J. Alloys. Compd.* **2021**, *872*, 159746. [CrossRef]
22. Kundu, S.; Roy, S.K.; Banerji, P. GaAs Metal–Oxide–Semiconductor Device with Titanium Dioxide as Dielectric Layer: Effect of Oxide Thickness on the Device Performance. *J. Phys. D Appl. Phys.* **2011**, *44*, 155104. [CrossRef]
23. Orlianges, J.-C.; Crunteanu, A.; Pothier, A.; Merle-Mejean, T.; Blondy, P.; Champeaux, C. Titanium Dioxide Thin Films Deposited by Pulsed Laser Deposition and Integration in Radio Frequency Devices: Study of Structure, Optical and Dielectric Properties. *Appl. Surf. Sci.* **2012**, *263*, 111–114. [CrossRef]
24. Batool, S.; Imran, Z.; Rafiq, M.; Hasan, M.; Willander, M. Investigation of Dielectric Relaxation Behavior of Electrospun Titanium Dioxide Nanofibers Using Temperature Dependent Impedance Spectroscopy. *Ceram. Int.* **2013**, *39*, 1775–1783. [CrossRef]
25. Cho, D.; Naydich, A.; Frey, M.W.; Joo, Y.L. Further Improvement of Air Filtration Efficiency of Cellulose Filters Coated with Nanofibers via Inclusion of Electrostatically Active Nanoparticles. *Polymer* **2013**, *54*, 2364–2372. [CrossRef]
26. Bonino, C.A.; Efimenko, K.; Jeong, S.I.; Krebs, M.D.; Alsberg, E.; Khan, S.A. Three-Dimensional Electrospun Alginate Nanofiber Mats via Tailored Charge Repulsions. *Small* **2012**, *8*, 1928–1936. [CrossRef] [PubMed]
27. Liang, T.; Parhizkar, M.; Edirisinghe, M.; Mahalingam, S. Effect of Humidity on the Generation and Control of the Morphology of Honeycomb-like Polymeric Structures by Electrospinning. *Eur. Polym. J.* **2014**, *61*, 72–82. [CrossRef]

28. Megelski, S.; Stephens, J.S.; Chase, D.B.; Rabolt, J.F. Micro-and Nanostructured Surface Morphology on Electrospun Polymer Fibers. *Macromolecules* **2002**, *35*, 8456–8466. [CrossRef]
29. Rajendran, S.; Mahendran, O.; Kannan, R. Lithium Ion Conduction in Plasticized PMMA–PVdF Polymer Blend Electrolytes. *Mater. Chem. Phys.* **2002**, *74*, 52–57. [CrossRef]
30. Gayatri, R.; Fizal, A.N.S.; Yuliwati, E.; Hossain, M.S.; Jaafar, J.; Zulkifli, M.; Taweepreda, W.; Ahmad Yahaya, A.N. Preparation and Characterization of PVDF–TiO_2 Mixed-Matrix Membrane with PVP and PEG as Pore-Forming Agents for BSA Rejection. *Nanomaterials* **2023**, *13*, 1023. [CrossRef]
31. Boccaccio, T.; Bottino, A.; Capannelli, G.; Piaggio, P. Characterization of PVDF Membranes by Vibrational Spectroscopy. *J. Membr. Sci.* **2002**, *210*, 315–329. [CrossRef]
32. Ishihara, K.; Tsuji, T.; Sakai, Y.; Nakabayashi, N. Synthesis of Graft Copolymers Having Phospholipid Polar Group by Macromonomer Method and Their Properties in Water. *J. Polym. Sci. Part A Polym. Chem.* **1994**, *32*, 859–867. [CrossRef]
33. Gu, M.; Zhang, J.; Wang, X.; Ma, W. Crystallization Behavior of PVDF in PVDF-DMP System via Thermally Induced Phase Separation. *J. Appl. Polym. Sci.* **2006**, *102*, 3714–3719. [CrossRef]
34. Zhang, X.; Wang, Z.; Chen, M.; Liu, M.; Wu, Z. Polyvinylidene Fluoride Membrane Blended with Quaternary Ammonium Compound for Enhancing Anti-Biofouling Properties: Effects of Dosage. *J. Membr. Sci.* **2016**, *520*, 66–75. [CrossRef]
35. Hong, H.; Song, S.A.; Kim, S.S. Phase Transformation of Poly (Vinylidene Fluoride)/TiO_2 Nanocomposite Film Prepared by Microwave-Assisted Solvent Evaporation: An Experimental and Molecular Dynamics Study. *Compos. Sci. Technol.* **2020**, *199*, 108375. [CrossRef]
36. Li, Y.; Yin, X.; Si, Y.; Yu, J.; Ding, B. All-Polymer Hybrid Electret Fibers for High-Efficiency and Low-Resistance Filter Media. *Chem. Eng. J.* **2020**, *398*, 125626. [CrossRef] [PubMed]
37. Shcherbachenko, L.; Borisov, V.; Maksimova, N.; Baryshnikov, E.; Karnakov, V.; Marchuk, S.; Ezhova, Y.V.; Ruzhnikov, L. Electret Effect and Electrotransport in Disperse Organic and Inorganic Systems. *Tech. Phys.* **2009**, *54*, 1372–1379. [CrossRef]
38. Ko, W.-C.; Tseng, C.-K.; Wu, W.-J.; Lee, C.-K. Charge Storage and Mechanical Properties of Porous PTFE and Composite PTFE/COC Electrets. *e-Polymers* **2010**, *10*, 032. [CrossRef]
39. Handa, A.; Baptista, R.M.F.; Santos, D.; Silva, B.; Rodrigues, A.R.O.; Oliveira, J.; Almeida, B.; de Matos Gomes, E.; Belsley, M. Electrospun Microstructured Biopolymer Fibers Containing the Self-Assembled Boc–Phe–Ile Dipeptide: Dielectric and Energy Harvesting Properties. *Sustainability* **2023**, *15*, 16040. [CrossRef]
40. Hung, C.-H.; Leung, W.W.-F. Filtration of Nano-Aerosol Using Nanofiber Filter under Low Peclet Number and Transitional Flow Regime. *Sep. Purif. Technol.* **2011**, *79*, 34–42. [CrossRef]
41. Li, P.; Wang, C.; Zhang, Y.; Wei, F. Air Filtration in the Free Molecular Flow Regime: A Review of High-Efficiency Particulate Air Filters Based on Carbon Nanotubes. *Small* **2014**, *10*, 4543–4561. [CrossRef] [PubMed]

Disclaimer/Publisher's Note: The statements, opinions and data contained in all publications are solely those of the individual author(s) and contributor(s) and not of MDPI and/or the editor(s). MDPI and/or the editor(s) disclaim responsibility for any injury to people or property resulting from any ideas, methods, instructions or products referred to in the content.